

# DeDop

Fully Adaptable and Configurable  
Altimeter Delay Doppler Processor

Sentinel 3 For Science - SAR Altimetry Studies  
SEOM Study 1.SARAE

Dedop Case Study Report  
ACDC Stability  
WP6700

Project ref.: DeDop\_ESA\_RP\_028  
Issue: 1.a  
03/12/2017  
Activity: SEOM SARAE



This page has been intentionally left blank



## Change Record

Date	Issue	Section	Page	Comment
27/11/2017	0.a	all	all	first issue
03/12/2017	0.b	all	all	general revision
05/12/2017	1.a	all	all	general revision

Table 1: Change Record

## Control Document

Process	Name	Date
Written by:	Chris Ray	03/12/2017
Checked by:	Eduard Makhoul Varona	04/12/2017
Approved by:	Mònica Roca	??

Subject	DeDop Case Study N	Project	SARAE (DeDop)
Author	Organization	Internal References	
Chris Ray	isardSAT		

	Signature	Date
For DeDop Team		
For ESA		

Table 2: Control Document



## Contents

<b>1</b>	<b>Introduction</b>	<b>6</b>
1.1	Purpose . . . . .	6
1.2	Document Structure . . . . .	6
1.3	Acronyms . . . . .	6
1.4	References . . . . .	6
<b>2</b>	<b>Case Study Description</b>	<b>6</b>
2.1	Scientific/Technical Context . . . . .	6
2.2	Objective of Case Study . . . . .	6
2.2.1	DeDop Goals . . . . .	6
2.2.2	Technical Goals . . . . .	7
2.3	Input Data Sets . . . . .	8
2.4	DeDop Tool Processing Specifications . . . . .	8
2.5	Additional Post DeDop Processing . . . . .	8
2.5.1	Stability of Simple Retracker . . . . .	8
2.5.2	Estimate of region of known stability . . . . .	9
2.5.3	Methodology . . . . .	9
<b>3</b>	<b>Analysis of Case Study Output</b>	<b>11</b>
3.1	Technical Results . . . . .	11
3.1.1	Mean number of steps to converge . . . . .	11
3.1.2	Prevalence and value of divergent initial conditions . . . . .	11
3.2	Impact of Different DeDop Processing Configurations . . . . .	15
3.3	DeDop Processor and Tool Performance . . . . .	15
<b>4</b>	<b>Conclusions/ Recommendations</b>	<b>15</b>
4.1	Technical Study . . . . .	15
4.2	DeDop User Experience Study . . . . .	15
<b>A</b>	<b>Presentation of case study: File name</b>	<b>16</b>



## List of Figures

1	A conceptual diagram of paths of two sequences $p_n$ in the parameter space. The two paths start with different initial locations $p_0$ . One path converges to a limiting value $p_\infty$ and the other does not. . . . .	7
2	A conceptual diagram of the regions with common convergence points. . . . .	7
3	Here is the scatter of $p_\infty$ for 300 consecutive DDMs of a Cryosat track on the 2 January 2013 over the pacific for which $\langle H_s \rangle = 4.2\text{m}$ . We have taken the mean of the 300 $p_\infty$ values to be the value of $p_{ss}$ . In the second graph we have used this estimated $p_{ss}$ to scale the parameters. A vertical axis is a log scale with $p_{ss}$ as the reference value, while the horizontal axis is offset by $k_{ss}$ . Using this scaling method leads to a fairly consistent scatter across different sea states. . . . .	9
4	Here is the grid of initial values $p_0^{i,j}$ for the sequences. . . . .	10
5	This is the histograms of the number of steps to converge for two different initial conditions $(g, k)$ for all the DDM's in a track. The track has a mean significant wave height of $\langle H_s \rangle = 2.6\text{m}$ and is the same track as in figure 6. . . . .	10
6	This is a contour plot of the mean number of steps and the relative standard deviation of steps for the entire domain of initial conditions $(g, k)$ . The mean is over all the DDM's in a track, the same track is in figure 5. The mean significant wave height over this track was $\langle H_s \rangle = 2.6\text{m}$ . The value (7.0 and 2.9) of the left plot at the obscured rectangles is the mean of the data in the histograms in figure 5, while the value (1.3/7.0 and 0.6/2.9) at the obscured rectangles in the right plot is the ratio of the standard deviation and mean of the data in figure 5. . . . .	11
7	Graph of the percentage that diverged for each different $p_0$ for those DDMs in the $H_s = 1.3\text{m}$ and $1.8\text{m}$ bins. . . . .	12
8	This is the histograms of the number of steps to converge for two different initial conditions $(g, k)$ for all the DDM's in a track with $\langle H_s \rangle = 1.5\text{m}$ . The histogram on the left shows a distribution that who's tail goes all the way to 40, the threshold set for convergence. This implies that there were probably some sequences that did not converge in 40 steps that would have if the threshold were set higher. . . . .	12
9	The mean number of steps bin sorted by $H_s$ . In the lower left corner is the ratio of the number divergent sequences and the number of sequences. . . . .	13
10	The graph shows the relative standard deviation of the number of steps. . . . .	14

## List of Tables

1	Change Record . . . . .	3
2	Control Document . . . . .	3



# 1 Introduction

## 1.1 Purpose

The purpose of this document is to report on the results of a study of the stability of the ACDC algorithm and to report on my experience of attempting to use DeDop for the first time and DeDop's effectiveness for the purposes of this study.

In brief, the ACDC algorithm is a method of synthetic aperture radar altimetry used to reduce the effects of speckle noise in the multi-looked backscattered power waveform. The ACDC algorithm is a means of forming a waveform from the delay-doppler map (DDM), but the algorithm requires an estimate of the significant wave height  $H_s$  and the sea surface height  $h$  in order to form the ACDC waveform from the DDM. Thus in order to retrack the ACDC waveform to estimate  $H_s$  and  $h$  one needs to start with an initial estimate for these two geophysical parameters. We represent the ACDC processing that leads to an estimate of the geophysical parameters by the operator  $\Xi$  acting on a vector of parameters  $p = [H_s, h]$  and the DDM  $\psi$ .

$$p_{\text{new estimate}} = \Xi(p_{\text{initial estimate}}, \psi) \quad (1)$$

In this way the algorithm is iterative in nature. One hopes that the new estimate of the geophysical parameters is closer than the initial estimate to the geophysical parameters of the sea from which the echo returned. The goal of this investigation is to see if this hope is justified, if the ACDC algorithm is stable.

## 1.2 Document Structure

The document structure is well represented by the table of contents.

## 1.3 Acronyms

DDM	Delay doppler map
ACDC	Amplitude Compensation and Dilation Compensation

## 1.4 References

*IEEE Geoscience and Remote Sensing Letters*, Volume 12, No. 12, p2473, December 2015. Digital Object Identifier 10.1109/LGRS.2015.2485119.

# 2 Case Study Description

## 2.1 Scientific/Technical Context

The ACDC algorithm is a under investigation for it potential usefulness in make more precise measurements of the sea surface height and the significant wave height. It is potentially more precise because the method has been shown to produce retracked geophysical parameters with lower variation than the retrack parameters of the conventional delay-doppler processor. While there has been indications that the ACDC algorithm is stable there has been no careful analysis over a broad range of conditions. This study is intended to do that analysis.

## 2.2 Objective of Case Study

### 2.2.1 DeDop Goals

The primary objective of the study was to see how difficult it is for an "outsider" to extend the DeDop tool.

### 2.2.2 Technical Goals

The secondary objective is to see if the ACDC algorithm is stable, this objective will be stated more carefully here.

Suppose we make a sequence of estimates  $p_n$  starting from an initial estimate  $p_0$ :

$$p_n = \Xi(p_{n-1}, \psi) = \Xi^n(p_0, \psi) \quad (2)$$

where we use the notation  $\Xi^n$  to represent the iteration  $n$  times of the  $\Xi$  so that for example  $\Xi^2(p_0, \psi) = \Xi(\Xi(p_0, \psi), \psi)$ . The questions that need to answer can be stated as follows.

- **First:** For what values of  $p_0$  does the sequence  $p_n$  converge to a limiting value? If the limit exists we call it  $p_\infty$ .

$$p_\infty = \lim_{n \rightarrow \infty} p_n = \lim_{n \rightarrow \infty} \Xi^n(p_0) \quad (3)$$

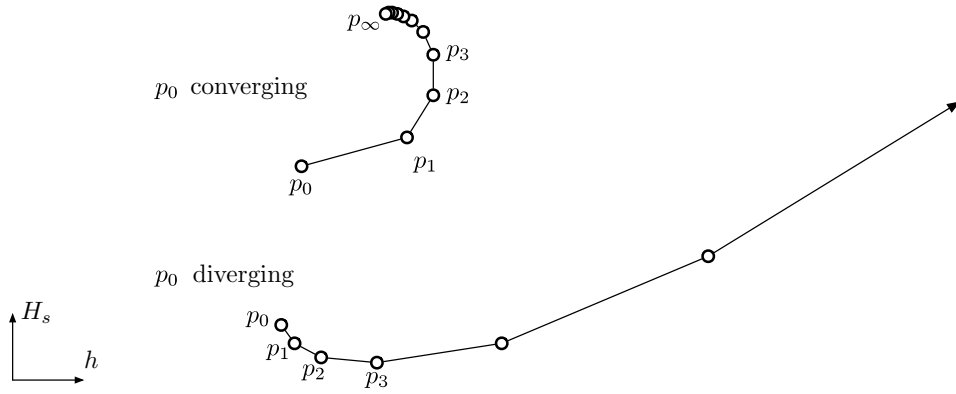


Figure 1: A conceptual diagram of paths of two sequences  $p_n$  in the parameter space. The two paths start with different initial locations  $p_0$ . One path converges to a limiting value  $p_\infty$  and the other does not.

- **Second:** For those  $p_0$  that do converge, do they converge to the same value of  $p_\infty$ ? We can divide the two dimensional  $(h, H_s)$  parameter space into mutually exclusive regions. Figure 2 is a conceptual depiction of such regions: all the points  $p$  in the yellow region  $R_a$  converge to the value  $p_\infty^a$ , while all the points in the gray region  $R_\emptyset$  do not converge to any point.

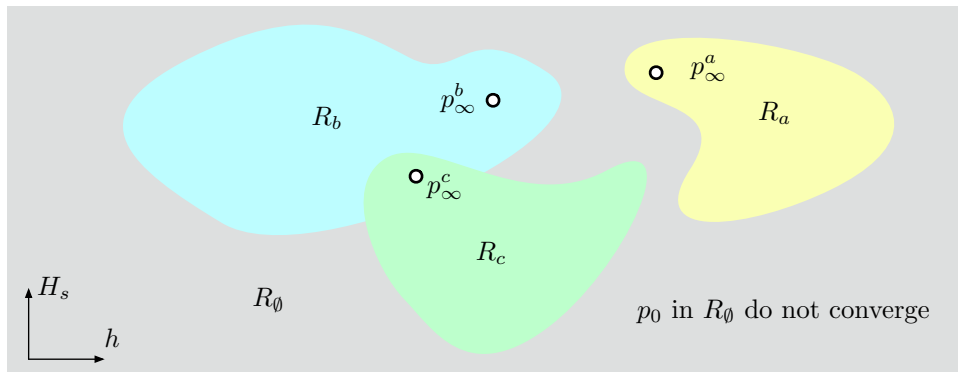


Figure 2: A conceptual diagram of the regions with common convergence points.



## 2.3 Input Data Sets

The input data set was Cryosat data from January of 2013 over a patch of the South Pacific from the French Polynesia to the coast of South America: between -5 and -25 degrees latitude and -85 and -138 degrees longitude.

## 2.4 DeDop Tool Processing Specifications

There was not sufficient flexibility in the processor specifications in order to allow for the processing of the L1b data that was needed for this case study. This was anticipated from the beginning. The intention was to see how difficult it is for an “outsider” to extend the DeDop tool. Unfortunately the task was much larger than anticipated. After spending four times the contracted time in trying to learn the DeDop system and the associated systems it was necessary to do the computations for the case study from the L1b data directly in order to be able to finish the technical part of the case study. The DeDop tool was not used in the analysis.

## 2.5 Additional Post DeDop Processing

Here the processing that was used in the study is described.

Internal to the model are two parameters  $g$  and  $k$  that are tracked instead of the significant wave height  $H_s$  and sea surface height  $h$ . This is so for computational efficiency since there is a one-to-one algebraic relationship between  $H_s$  and  $g$  and  $H_s$  only enters the model through the range scaling parameter  $g$ . In a similar way  $h$  only enters the model through the parameter  $k$  (the epoch).

For the remainder of this document the mappings  $H_s \leftrightarrow g$  and  $h \leftrightarrow k$  will be assumed, so while  $g$  is not the significant wave height it can be thought of as the parameter used to compute the significant wave height, likewise  $k$  can be thought of as the parameter that determines the sea surface height.

### 2.5.1 Stability of Simple Retracker

The ACDC method would not have been investigated very far at all if there was not some indication that the algorithm was stable, and indeed it has been shown that the method is stable if  $p_0$  is not too far from the value  $p_{ss}$  of the actual sea state. Consider the following simple ACDC retracker. Start with an initial guess  $p_\infty^0$  and use this with the first DDM  $\psi^1$  in the track to make a first estimate, where the upper index refers to the DDM number.

$$p_1^1 = \Xi(p_\infty^0, \psi^1) \quad (4)$$

and so repeating we find the sequence of estimates for DDM 1.

$$p_n^1 = \Xi^n(p_\infty^0, \psi^1) \quad (5)$$

This can be repeated with the second DDM, but this time using the limiting value  $p_\infty^1$  of the first DDM as the initial estimate for the second DDM.

$$p_n^2 = \Xi^n(p_\infty^1, \psi^2) \quad (6)$$

Indeed this can be repeated until the end of the track.

$$p_n^m = \Xi^n(p_\infty^{m-1}, \psi^m) \quad (7)$$

We see that the simple tracker method is to let  $p_0^m = p_\infty^{m-1}$ . This approach depends on the assumption that the sea state in one DDM will not be very different from the sea state of the previous DDM in the track. The above method simple retracker has been used extensively in the development of the ACDC method and has been found to be stable except in cases of artifacts in the DDM from such things as point scatterers or  $\sigma_0$  blooms. In this investigation we will see how far  $p_0$  can deviate from  $p_{ss}$  before the method no longer returns us to the region of  $p_{ss}$ .



### 2.5.2 Estimate of region of known stability

Because of speckle noise in the returned power, each DDM will have variations from the expected mean power from the particular sea being measure. These variation cause variations in the estimated sea state parameters returned from the simple retracker, as seen in figure 3. So that for a particular DDM the value of  $p_\infty$  will not be equal to  $p_{ss}$  for the actual sea state. We will assume that the mean value of  $p_\infty^m$  over a short section of DDMs corresponds to the value of  $p_{ss}$  for the sea imaged by those DDMs (up to tracker bias of course).

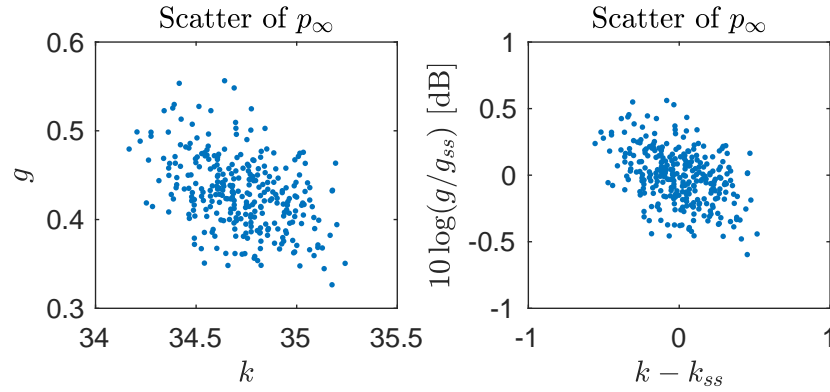


Figure 3: Here is the scatter of  $p_\infty$  for 300 consecutive DDMs of a Cryosat track on the 2 January 2013 over the pacific for which  $\langle H_s \rangle = 4.2\text{m}$ . We have taken the mean of the 300  $p_\infty$  values to be the value of  $p_{ss}$ . In the second graph we have used this estimated  $p_{ss}$  to scale the parameters. A vertical axis is a log scale with  $p_{ss}$  as the reference value, while the horizontal axis is offset by  $k_{ss}$ . Using this scaling method leads to a fairly consistent scatter across different sea states.

In the simple ACDC retracker described above the input guess has been off by roughly the width of the parameter scatter caused by the speckle. We can see this through the defining relationship of the simple retracker method  $p_0^m = p_\infty^{m-1}$ , because this implies that error in our initial guess is

$$|p_0^m - p_\infty^m| = |p_\infty^{m-1} - p_\infty^m| \quad (8)$$

Thus the error in our initial guesses is the distance between successive  $p_\infty$ . In figure 3 the width of the scatter is roughly 1dB in  $g$  and 1 lag in  $k$ . This size scatter is typical.

With this level of error in  $p_0$  the ACDC method has in practice been stable. Thus we feel safe in assuming that regions around  $p_{ss}$  of the above diameter are within the convergent region of  $p_{ss}$ . What remains to be investigated is the convergence outside of this close region.

### 2.5.3 Methodology

- For each track the simple ACDC retracker was applied, giving a reasonable estimate of  $p_\infty$  for each DDM in the track.
- For each DDM a grid of initial values  $p_0^{i,j} = (g_0^{i,j}, k_0^{i,j})$  centered on  $p_\infty$  with steps of size 1 dB in  $g$  and 1 lag in  $k$  was created. This grind is shown in fig.4.

$$\begin{aligned} g_0^{i,j} = g_\infty 10^{i/10} &\longrightarrow 10 \log_{10} \left( \frac{g_0^{i,j}}{g_\infty} \right) = i \longrightarrow \frac{g_0^{i,j}}{g_\infty} = 10^{i/10} \text{ dB} \\ k_0^{i,j} = j + k_\infty &\longrightarrow k_0^{i,j} - k_\infty = j \longrightarrow \Delta k_0^{i,j} = j \end{aligned} \quad (9)$$

We will use the notation  $\Delta k = k - k_\infty$ .

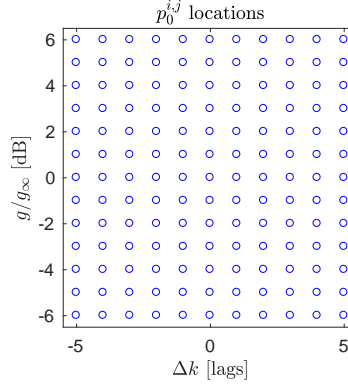


Figure 4: Here is the grid of initial values  $p_0^{i,j}$  for the sequences.

- For each of the  $p_0^{i,j}$  in the grid, the sequence  $p_n^{i,j}$  was computed via  $p_n^{i,j} = \Xi^n(p_0^{i,j})$  until either  $n > 40$  or both

$$\left| 10 \log_{10} \left( \frac{g_n^{i,j}}{g_\infty} \right) \right| < 0.5 \quad \text{and} \quad |k_n^{i,j} - k_\infty| < 0.5 . \quad (10)$$

- We take the final  $n$  as the number of steps  $N^{i,j}$  required to reach the known convergent region from the initial location  $p_0^{i,j}$ . If  $n > 40$  we consider this sequence as having diverged and we set  $D^{i,j} = 1$  otherwise we set  $D^{i,j} = 0$ .

At this point we have a matrix of steps  $N^{i,j}$  and a count of record of divergence  $D^{i,j}$  for each DDM. An example of view of a collection of these  $N^{i,j}$  over a track of DDM's is represented in the histograms of figure 5, and in figure 6 is the mean number of steps  $\langle N^{i,j} \rangle$  over the track of the number of steps  $N^{i,j}$ . It is worth studying figures 5 and 6 and the relationship between the two in order to fully understand the remainder of this report. In figure 7 is shown the percentage that diverged,  $100\langle D^{i,j} \rangle$ .

- The DDM's are bin sorted by significant wave height. Then the average number of steps  $\langle N^{i,j} \rangle$  and standard deviation of the number of steps  $\sigma^{i,j}$  are computed for each bin.

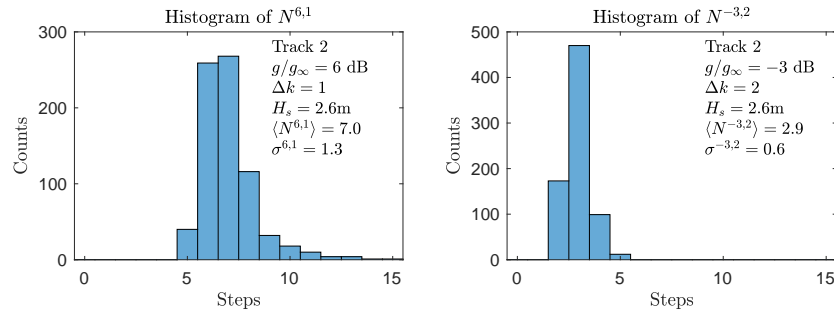


Figure 5: This is the histograms of the number of steps to converge for two different initial conditions  $(g, k)$  for all the DDM's in a track. The track has a mean significant wave height of  $\langle H_s \rangle = 2.6$  m and is the same track as in figure 6.

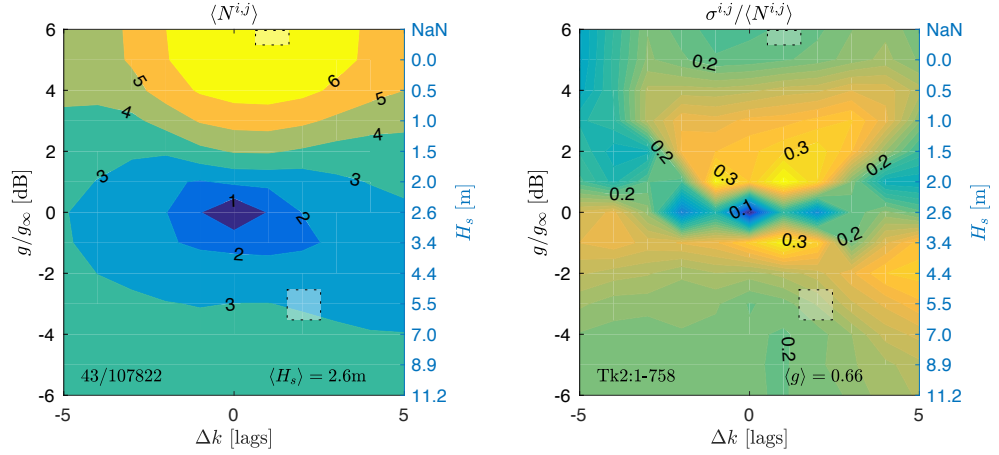


Figure 6: This is a contour plot of the mean number of steps and the relative standard deviation of steps for the entire domain of initial conditions  $(g, k)$ . The mean is over all the DDM's in a track, the same track is in figure 5. The mean significant wave height over this track was  $\langle H_s \rangle = 2.6\text{m}$ . The value (7.0 and 2.9) of the left plot at the obscured rectangles is the mean of the data in the histograms in figure 5, while the value (1.3/7.0 and 0.6/2.9) at the obscured rectangles in the right plot is the ratio of the standard deviation and mean of the data in figure 5.

### 3 Analysis of Case Study Output

#### 3.1 Technical Results

##### 3.1.1 Mean number of steps to converge

Figure 5 shows the histograms of the number of steps  $N^{6,1}$  and  $N^{-3,2}$  for all the DDM's in a track with  $\langle H_s \rangle = 2.6\text{m}$ . The histogram indicates that for a particular initial condition  $(i, j)$  the sequence converges in a fairly well defined number of steps, this in turn implies that the distribution of steps is fairly well represented by the mean  $\langle N^{i,j} \rangle$  and standard deviation  $\sigma^{i,j}$  of the number of steps.

Figure 6 is the mean number of steps required to converge to  $p_{\infty}$  over the entire parameter space of initial conditions for the same track. In figure 9 we see something similar but it is the mean number of steps over all tacks, bin sorted by significant wave height values, with the mean performed per bin.

The primary observation here is that for the entire region studied ( $\pm 6\text{dB}$  in  $\frac{g}{g_{\infty}}$  and  $\pm 5$  lags in  $\Delta k$ ) all initial conditions converge to the same  $p_{\infty}$ , so that the ACDC method is stable even with a grossly inaccurate initial guess. Note that a 12dB range in  $g$  leads to a range in significant wave height of approximately 0 to 20 meters, so that the region of study is sufficiently complete.

##### 3.1.2 Prevalence and value of divergent initial conditions

In the lower left corner of each graph of figure 6 and 9 is the ration of the number of initial points  $p_0$  that did not converge and the number of initial points. For significant wave heights greater than 2.5m there were no instances of divergence. For significant wave height less than 2.5m there were divergences. To see for which initial values  $p_0^{i,j}$  the sequence diverges, the percentage that diverged  $100\langle D^{i,j} \rangle$  is graphed in figures 7 for conditions that had a significant number of divergences. By comparing these graphs with the bottom two graphs in figure 9 it can be seen that the  $p_0$  that require a large number of steps to converge, also lead to the largest percentage of divergences, which is not surprising. In all cases the divergences occur for  $p_0$  with significant wave heights less than  $H_s$ , and if the initial guess was always taken with the estimated significant wave height

greater than 2.0 meters there would have been no divergences. This seems an important observation about the method.

Another thing that becomes apparent is that the greatest percentage of divergence is for sea states with lower significant wave height. For a significant wave height of 1.3m up to 9% of the sequences diverged if the initial guess for significant wave height was below 0.8m.

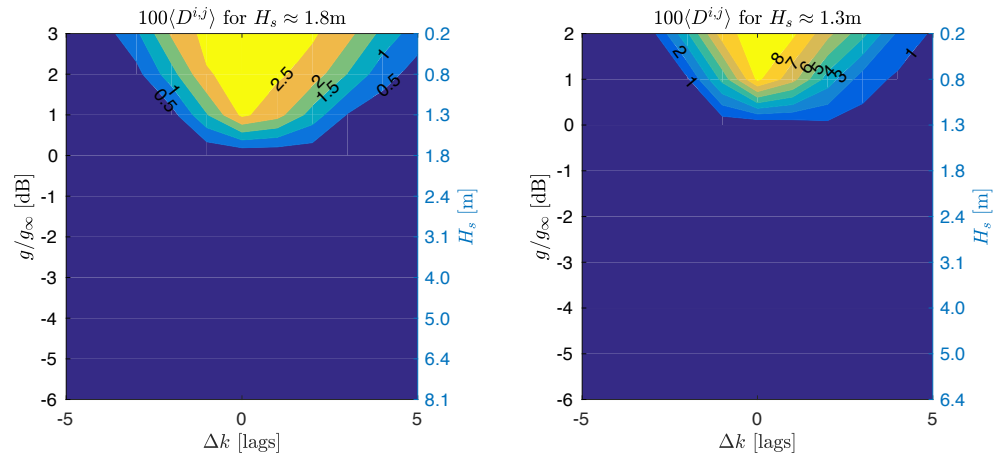


Figure 7: Graph of the percentage that diverged for each different  $p_0$  for those DDMs in the  $H_s = 1.3\text{m}$  and  $1.8\text{m}$  bins.

Figure 8 shows the histogram of number of steps to converge for a track with significant wave height of 1.5m. Because the distribution evident in the histogram reaches the edge of our upper limit (40), it would appear that there were some DDM's that would have converged if the program did not give up at 40 steps. Even so in figure 5 we see a similar histogram for a track with significant wave height of 2.6m. In figure 5 the distribution falls well short of the 40 step limit so there is no indication that the 40 step limit was not sufficiently close to infinity. Nevertheless 43 of the 107822 sequences (0.04%) did not converge. So the lack of convergence is not only due to the fact that  $40 \neq \infty$ : when the initial estimate of significant wave height is too low some DDM's have sequences that do not converge.

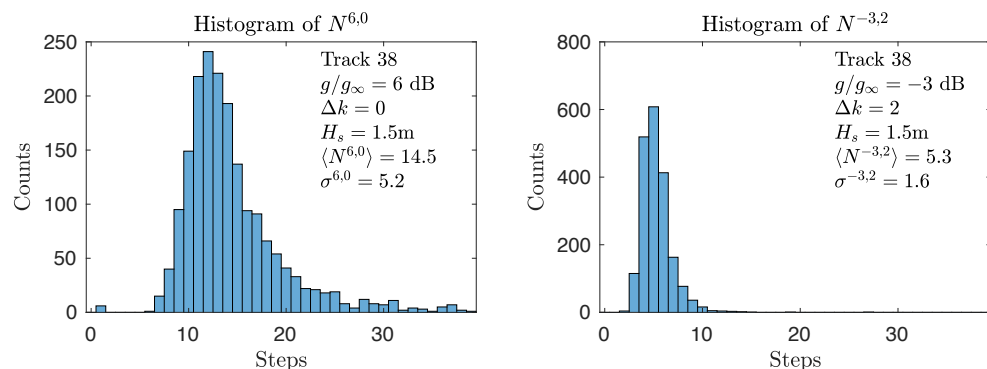


Figure 8: This is the histograms of the number of steps to converge for two different initial conditions  $(g, k)$  for all the DDM's in a track with  $\langle H_s \rangle = 1.5\text{m}$ . The histogram on the left shows a distribution that who's tail goes all the way to 40, the threshold set for convergence. This implies that there were probably some sequences that did not converge in 40 steps that would have if the threshold were set higher.

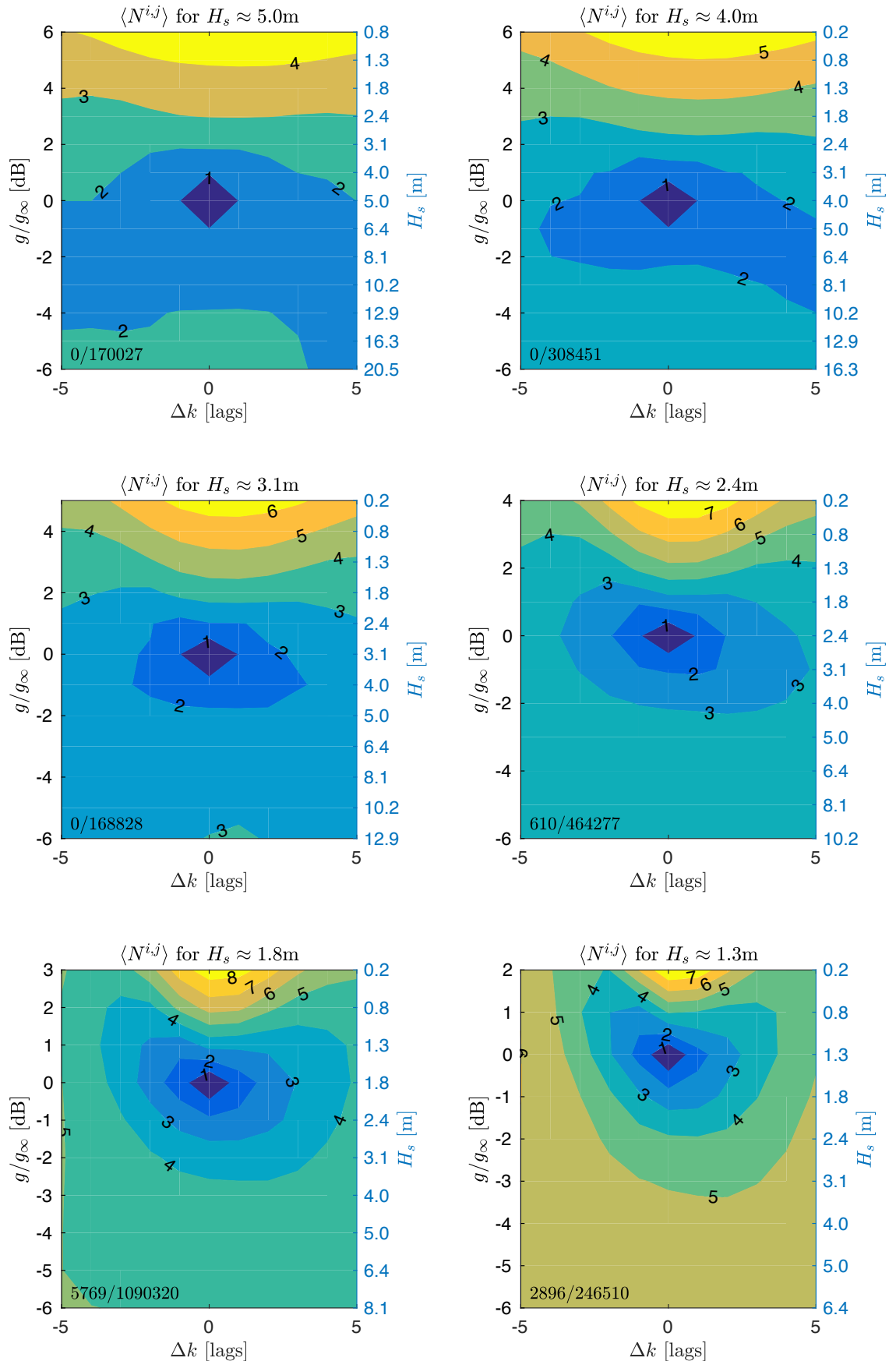


Figure 9: The mean number of steps bin sorted by  $H_s$ . In the lower left corner is the ratio of the number divergent sequences and the number of sequences.

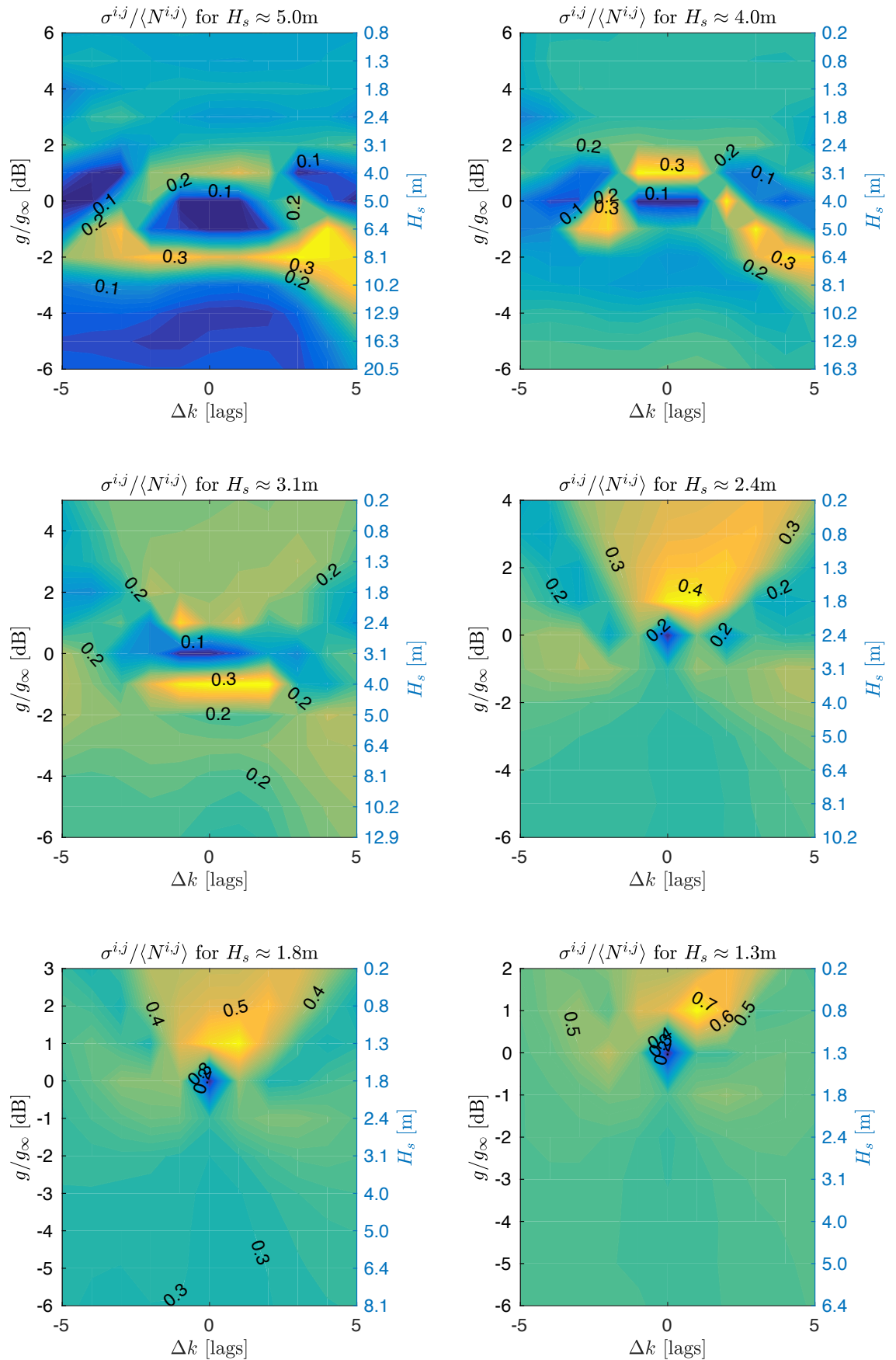


Figure 10: The graph shows the relative standard deviation of the number of steps.



### 3.2 Impact of Different DeDop Processing Configurations

I would recommend including the option in the DeDop configuration of having FFT windowing in range in the same way there is the option for azimuth windowing.

### 3.3 DeDop Processor and Tool Performance

I did not run a sufficient amount of data with the DeDop tool to be able to compare the performance with other systems.

## 4 Conclusions/ Recommendations

The conclusions of the technical study and the conclusion of the DeDop user experience study will be presented separately.

### 4.1 Technical Study

- For 99.6% of initial estimates with  $0\text{m} < H_s < 20\text{m}$  and with the error in epoch less than five lags the ACDC algorithm converges toward to a single value  $p_\infty$ . The algorithm is stable over a broad range of initial conditions and DDM's.
- 100% of the sequences converged if the initial estimate of  $H_s$  was 2.0 meters or greater. For this reason it is suggested to use an initial estimate of  $H_s$  of at least 2.0 meters if there is not certainty that the actual value is lower.
- For the specific case of low significant wave height and an underestimate of this low significant wave height up to 8% of the sequences were found to diverge. This shows the importance of not underestimating the significant wave height when making the initial estimate.

### 4.2 DeDop User Experience Study

- The current DeDop documentation is sufficient to install DeDop tool from binary and process a track with the default settings. The configuration panel of DeDop Studio is nice, but without documentation on what the effect of the various flags will be, it is of limited use to anyone who did not write the code. One can of course try running with different flags set and see the results, but without understanding what is being done, the consequences of the action have little significance.
- Following the instructions provided in the DeDop installation guide and the associated installation guides for Miniconda and Github it was possible to install DeDop from source without too much fuss, except when the installation guide got out of sync with the evolving DeDop.
- There are quite a number of independent systems with which the user needs to be proficient in order to be able to extend the DeDop tool: Miniconda, Github, Python, a Python editor, Jupyter, and DeDop. Even with excellent documentation it takes some time to find one's bearings in a new environment. To this user all of the systems were unknown.
- The auto-generated documentation of the DeDop code is not particularly helpful in understanding the code. In browsing the code I was able to make very little headway in understanding the structure. It should be understood that I was new to Python when coming to this project, even so I have worked extensively in many languages. Perhaps to someone with previous Python experience the structure of the DeDop code would be self evident, but I still expect it would be difficult. If it was desired that others would extend DeDop I think human written documentation would be essential.



## **A Presentation of case study: File name**

The file DeDopWP6700slides.pdf has the slides for a presentation of the case study.